J Braz. Soc. Mech. Sci. Eng. (2017) 39:953–967
DOI 10.1007/s40430-016-0546-2

TECHNICAL PAPER

An exact solution for stability analysis of orthotropic rectangular thin plate under biaxial nonlinear in-plane loading resting on Pasternak foundation

Hosein Shahraki[1] · Fatemeh Farhatnia[2] · Mohammad Raeesi[3]

Received: 18 December 2015 / Accepted: 14 April 2016 / Published online: 7 May 2016

Abstract In this research, the buckling analysis of orthotropic rectangular plate resting on Pasternak elastic foundation was studied, using Frobenius exact solution method. The plate is subjected to biaxial in-plane loading with non-uniform distribution. It is assumed that it is simply supported by two opposite sides, and the remaining two edges can have any arbitrary conditions. To extract the governing equations on the buckling of the plate, the classical plate theory based on Kirchhoff hypothesis is employed. According to Levy solution, the buckling equation is reduced to an ordinary differential equation. Frobenius method is exploited in the governing equation, and the eigenvalue equation is obtained, imposing the boundary conditions on the other two sides. By solving the eigenvalue equation, the dimensionless critical buckling loads are determined. The accuracy of presented results is validated by comparing with available results in previous studies and also finite element method. Furthermore, the influences of some parameters such as aspect ratio, the ratio of elasticity modulus of the plate in two in-plane directions, the type of non-uniform loading in two states of uniaxial and biaxial loadings, various combinations of boundary conditions, lateral and shear stiffness coefficients of elastic foundation are examined on critical buckling.

Keywords Buckling analysis · Orthotropic plate · Pasternak elastic foundation · Biaxial loading · Frobenius method

1 Introduction

The applied structures in buildings, bridges, reservoir foundations, swimming pools, and various economic and industrial designs are formed from different components, of which the most important parts are plates. The plates in many structures are subjected to various tensile, bending, and compressive and shear loadings in various working conditions. In safe conditions, such loads cause buckling or static instability, which is very important in practice. A plate may be subjected to non-uniform load at the edges that can be applied as linear or nonlinear [1]. A comprehensive analysis was presented by Timoshenko and Gere [2] in which the linear and nonlinear buckling problems for plates with different forms under a variety of loadings and substantial presentation of the results of critical loads and buckling modes that are widely used in practical engineering design. Extensive studies about buckling of rectangular plates, being subjected to uniform in-plane loading, have been performed by Michelussi [3]. Leissa and Kang presented an exact solution for buckling analysis of a thin rectangular plate with two opposite simply-supported edges, using power series of Frobenius. In their work, the in-plane loading varies linearly along the edges. Additionally, they examined the vibration of an isotropic rectangular plate under linear load in another research [4, 5]. Javaheri and Eslami investigated the buckling of FGM

Technical Editor: Eduardo Alberto Fancello.

✉ Fatemeh Farhatnia
farhatnia@iaukhsh.ac.ir

[1] Young Researchers and Elite Club, Islamic Azad University (IAU), Khomeinishahr Branch, Boulevard Manzariye, Khomeinishahr, Isfahan 84174/119, Iran

[2] Faculty of Mechanical Engineering, Islamic Azad University, Khomeinishahr Branch, Khomeinishahr, Isfahan 84174/119, Iran

[3] Faculty of Civil Engineering, Islamic Azad University, Khomeinishahr Branch, Khomeinishahr, Isfahan 84174/119, Iran

plates under compressive plane load. They concluded that the critical buckling load for FGM plates increases as the ratio of width per length rises, and on the other hand, the critical load decreases as the ratio of width per thickness grows [6]. Bret and Devarakonda examined the buckling of rectangular plates with simply-supported boundary conditions at the edges which are subjected to sinusoidal loading, using Galerkin method [7]. The buckling of rectangular plates subjected to a variety of non-uniform loadings such as concentrated, local, sinusoidal, and other loadings was studied by Jana and Bhaskar [8, 9]. Wang et al. utilized the differential quadrature method to calculate the buckling load of rectangular plates which are subjected to non-uniform load at the edges. They examined cosine, linear, and parabolic shaped loads in the buckling load [10–12]. Hosseini-Hashemi applied Mindlin's plate theory to study isotropic rectangular plate buckling under in-plane loading with different boundary conditions [13]. Kumar Panda and Ramachandra investigated the buckling of composite plates subjected to non-uniform linear and parabolic shaped loadings at the edges, using shear deformation theory [14]. Latifi et al. examined the buckling of rectangular plates made of FGM in different boundary conditions and under biaxial compressive loading. The analysis is based on the classical plate theory with large deformations [15]. Abolghasemi et al, investigated the buckling of rectangular plates under non-uniform in-plane load, using the first-order shear deformation theory. The results were compared with the numerical solutions and those of the classical theory [16]. Orthotropic plates had high efficiency in civil infrastructure and other structural applications, because, they had such advantages as high stiffness ratio and resistance versus weight. Concrete slabs with reinforced asymmetric steel on both sides are examples of orthotropic plates. Harris presented the buckling analysis of orthotropic rectangular plates which were subjected to uniaxial and in-plane loadings in two directions [17]. Hwang and Lee analyzed the buckling of orthotropic plates under optional in-plane load. They examined the behavior of the plate under non-uniform loading with various boundary conditions, using the finite element method [18]. Lopatin and Morozov investigated the buckling analysis of orthotropic plate with CCFF boundary conditions. The problem was solved via partial differential equations and Galerkin method [19, 20]. Thai and Kim applied Levy solution to the buckling analysis of orthotropic plates, using two-variable refined plate theory [21]. Jafari and Eftekhari analyzed the buckling load and the natural frequencies of rectangular orthotropic plates located on elastic foundation for various types of loadings and boundary conditions, using a combination of Ritz and differential quadrature methods [22]. It is observed that one of the main conditions of the stability of a structure is providing appropriate support for the structure, the reaction of the structures on the foundation has long been considered. In Winkler model, the elastic foundation is independently modeled, using a series of springs. Despite the effectiveness of this model, the behavior of the elastic foundation is actually continuous, but it models the independent springs to analyze the behavior of the elastic foundation [23]. To correct this deficiency, researchers used Pasternak model, which is the most common one in this area, by adding a beam or plate with lateral shear stiffness [24]. Kim examined the stability and dynamic response of a thin infinite plate resting on Pasternak foundation [25]. Saeidifar and Sadeghi presented an analytical solution for the buckling analysis of rectangular plate under uniaxial compressive loading with changes in the thickness and modulus of elasticity in the y direction [26]. Akhavan et al. introduced an exact solution for the buckling analysis of Mindlin rectangular plates under uniform in-plane linear loading on elastic foundation, assuming two opposite simply-supported edges. To extract the governing equations, the analysis method is based on Mindlin theory, considering the effect of first-order shear deformation and interaction of plate-foundation. Moreover, in two other papers, they examined the analysis of free vibration of Mindlin rectangular plates under uniform in-plane linear loading [27, 28]. Hosseini-Hashemi et al. investigated hydrostatic vibration and buckling analysis of rectangular plates resting on Pasternak foundation and subjected to in-plane loads with linear variation for different boundary conditions [29]. Bodaghi and Saidi examined the buckling behavior of rectangular plates made of FGM materials on elastic Pasternak foundation under in-plane uniaxial linear and nonlinear loadings, based on the classical theory. Using Levy solution, the buckling equation was transformed to an ordinary differential equation with variable coefficients and then was solved exactly using power series of Frobenius method [30]. Panahandeh Shahraki et al., studied the buckling of FGM cracked plates supported by Pasternak foundation [31]. Foroughi and Azhari presented the buckling and free vibration of thick FGM plates resting on Pasternak elastic foundation, using finite strip method. The buckling analysis was carried out by normal finite strip method [32]. Yaghoobi and Fereidoon presented the analysis of mechanical and thermal buckling of FGM plate on elastic foundation, supposing shear deformation theory [33]. Viswanathana and Navaneethakrishnan investigated the buckling analysis of rectangular plate with variable thickness resting on elastic foundation, using spline approximation method [34]. Lam and Wang presented common exact solutions for elastic bending, buckling, and vibration of rectangular plate, using Levy solution on two-parametric elastic foundation via Green functions [35].

According to the abovementioned literature review, several works have been published on isotropic plate buckling under uniform uniaxial or biaxial loadings, whereas the buckling of orthotropic plate with non-uniform nonlinear loading is less considered, mainly due to the complexity of the solution process. This study introduces an exact analysis for the buckling of orthotropic rectangular plates based on the classical plate theory. It is assumed that a rectangular plate is resting on Pasternak (two-parametric) elastic foundation and is subjected to non-uniform in-plane biaxial loading. Using Levy resolution, the buckling equation is reduced to an ordinary differential equation with variable coefficients. It is solved using power series of Frobenius. By applying different combinations of boundary conditions along the opposite edge of the plate, the critical buckling load is obtained. The accuracy of results is confirmed by comparing them with those of previous studies as well as the finite element method. Also, the influences of parameters such as aspect ratio, the ratio of modulus of elasticity in two different directions, the type of non-uniform loading in both uniaxial and biaxial states, the various types of boundary conditions, the foundation coefficients on the critical buckling load of plate are examined.

2 Formulation presentation

Assume a rectangular thin plate with lateral dimensions of $a \times b$ and uniform thickness of h, as shown in Fig. 1, which is simply supported at $x = 0$, a while the other two edges of $y = 0$, b have any arbitrary conditions such as the clamped (C), and simply (S) or free support (F). It is assumed that the material is orthotropic, and the main orthotropic directions are in the directions of x and y-axes. Shear modulus G of the plate and the relationship between four independent elastic constants can be expressed as follows [1]:

$$G \approx \frac{\sqrt{E_x E_y}}{2\left(1+\sqrt{\upsilon_x \upsilon_y}\right)}, \qquad \frac{\upsilon_x}{E_x} = \frac{\upsilon_y}{E_y}. \tag{1}$$

In the plane stress condition, bending and torsional stiffness of the orthotropic plate is defined as follows [1]:

$$\begin{aligned} D_{11} &= \frac{E_x h^3}{12\left(1-\nu_{xy}\nu_{yx}\right)}, \quad D_{12} = D_{21} = \frac{E_x \nu_{yx} h^3}{12\left(1-\nu_{xy}\nu_{yx}\right)} \\ D_{22} &= \frac{E_y h^3}{12\left(1-\nu_{xy}\nu_{yx}\right)}, \quad D_{66} = \frac{G_{xy} h^3}{12}. \end{aligned} \tag{2}$$

The governing equation in the buckling of orthotropic rectangular plate under biaxial in-plane loading, regardless of the shear force N_{xy} per unit of the length, which rests on Pasternak elastic foundation is as follows [30]:

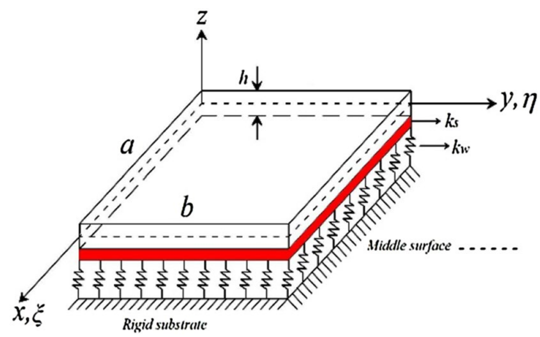

Fig. 1 Orthotropic rectangular plate resting on Pasternak elastic foundation

$$\begin{aligned} &D_{11}\frac{\partial^4 w}{\partial x^4} + 2(D_{12}+2D_{66})\frac{\partial^4 w}{\partial x^2 \partial y^2} \\ &+ D_{22}\frac{\partial^4 w}{\partial y^4} + K_w.w - K_s\left(\frac{\partial^2 w}{\partial x^2} + \frac{\partial^2 w}{\partial y^2}\right) \\ &- N_x\frac{\partial^2 w}{\partial x^2} - N_y\frac{\partial^2 w}{\partial y^2} = 0, \end{aligned} \tag{3}$$

where K_w and K_s are the coefficients of lateral and shear stiffness of the foundation, respectively. W, N_x, N_y are out-plane displacement, and the normal forces per unit of the length along x and y directions, respectively. To make a dimensionless form of the governing Eq. (3), the following parameters are defined as follows:

$$\begin{aligned} &\xi = \frac{x}{a}, \quad \eta = \frac{y}{b} \qquad \frac{\partial \xi}{\partial x} = \frac{1}{a}, \quad \frac{\partial \eta}{\partial y} = \frac{1}{b} \\ &\frac{\partial w}{\partial x} = \frac{\partial w}{\partial \xi}\frac{\partial \xi}{\partial x} = \frac{\partial w}{\partial \xi}\left(\frac{1}{a}\right) \qquad \frac{\partial w}{\partial y} = \frac{\partial w}{\partial \eta}\frac{\partial \eta}{\partial y} = \frac{\partial w}{\partial \eta}\left(\frac{1}{b}\right). \end{aligned} \tag{4}$$

Based on Levy approach, the following expansions of displacements are chosen as follows by considering that the two opposite sides of the plate are simply supported in x direction:

$$w(\eta, \xi) = Y_m(\eta)\sin(m\pi\xi), \tag{5}$$

where Y_m is a function of η, and m is the number of half-waves of the shape modes in x direction. This function satisfies boundary conditions in $\xi = 0$, 1. Substituting the parameters of Eqs. (4) and (5) in (3), and arranging it based on the order of Y_m, the following equation can be obtained:

$$\begin{aligned} &D_{22}\left(\frac{1}{b}\right)^4 Y_m^{IV} + \left[-2(D_{12}+2D_{66})\left(\frac{m\pi}{ab}\right)^2 - K_s\left(\frac{1}{b^2}\right) - N_y\left(\frac{1}{b^2}\right)\right]Y_m'' \\ &+ \left[D_{11}\left(\frac{m\pi}{a}\right)^4 + K_w + K_s\left(\frac{m\pi}{a}\right)^2 + N_x\left(\frac{m\pi}{a}\right)^2\right]Y_m = 0. \end{aligned} \tag{6}$$

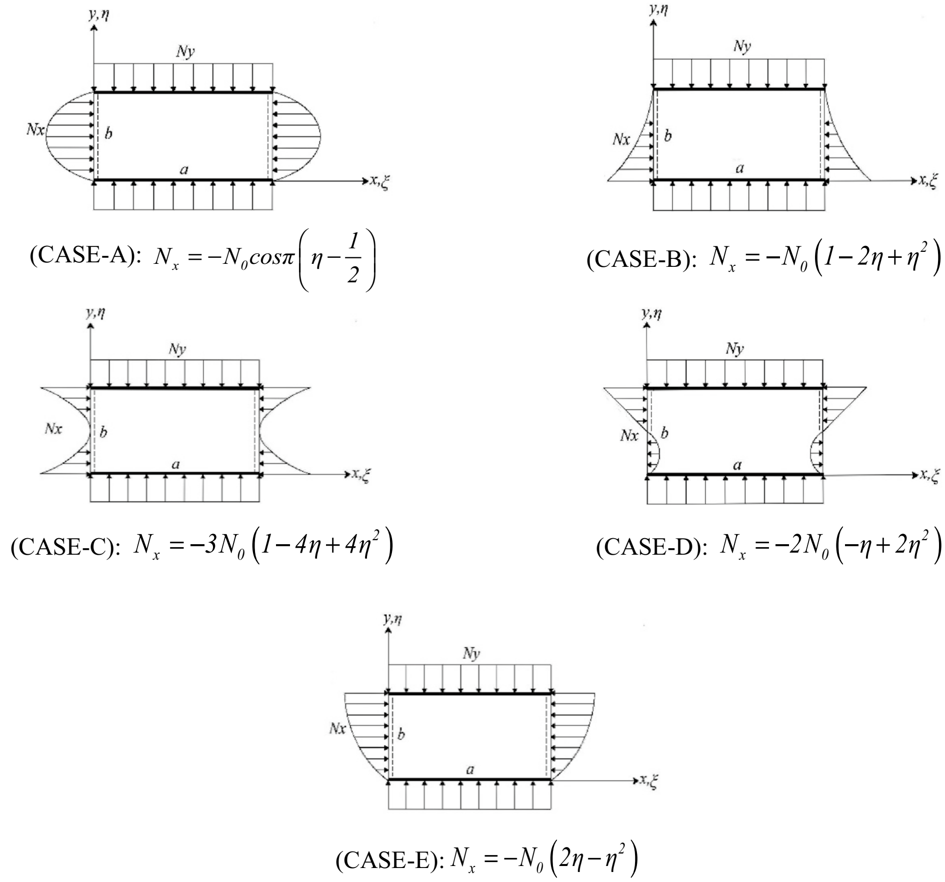

Fig. 2 Schematic of non-uniform loading cases of in-plane loading with boundary condition SCSC

2.1 Orthotropic rectangular plate under biaxial loading

In this section, various types of non-uniform loading are examined, and the governing differential equations of plate buckling are solved by Frobenius method. The distribution of in-plane loading per unit length in direction x is considered as follows:

$$N_x = -\mu N_0\left(a_0 + a_1\eta + a_2\eta^2 + a_3\eta^3 + a_4\eta^4 + a_5\eta^5\right), \tag{7}$$

where a_1, a_2, a_3, a_4, and a_5 are determined as dependent on the type of loading. N_0 is the maximum intensity of the in-plane load per unit length. The loading in y direction is defined in the form of the mean function of loading in x direction with proportion coefficient (R) as Eq. (8):

$$\begin{aligned} &N_y = R\bar{N}_x, \quad \bar{N}_x = \frac{1}{b}\int_0^b N_x \mathrm{d}y = \int_0^1 N_x \mathrm{d}\eta \\ &N_y = -R\mu N_0\left(a_0 + \frac{a_1}{2} + \frac{a_2}{3} + \frac{a_3}{4} + \frac{a_4}{5} + \frac{a_5}{6}\right). \end{aligned} \tag{8}$$

In this study, five cases of loading are examined according to Fig. 2. Also, the coefficients of a_i and μ can be seen for each case in Table 1.

2.2 Applying Frobenius method to governing equations

Suppose that the rectangular plate is under in-plane loading according to Fig. 2 in both x and y directions. N_0 is the intensity of compressive force (load factor per length unit). In general, to solve the governing equation by substituting Eqs. (7) and (8) in (6), the following equation can be obtained:

$$\begin{aligned} &D_{22}\left(\frac{1}{b}\right)^4 Y_m^{IV} + \left[-2(D_{12} + 2D_{66})\left(\frac{m\pi}{ab}\right)^2 - \frac{K_s}{b^2} + \frac{N_0 R\mu}{b^2}\left(a_0 + \frac{a_1}{2} + \frac{a_2}{3} + \frac{a_3}{4} + \frac{a_4}{5} + \frac{a_5}{6}\right)\right] Y_m'' \\ &+ \left[D_{11}\left(\frac{m\pi}{a}\right)^4 + K_w + K_s\left(\frac{m\pi}{a}\right)^2 - \mu N_0\left(a_0 + a_1\eta + a_2\eta^2 + a_3\eta^3 + a_4\eta^4 + a_5\eta^5\right)\left(\frac{m\pi}{a}\right)^2\right] Y_m = 0. \end{aligned} \tag{9}$$

Table 1 Different types of loading rectangular plate

Load case	μ	a_0	a_1	a_2	a_3	a_4	a_5
CASE -A	1	$1-\frac{1}{8}\pi^2+\frac{1}{384}\pi^4$	$\frac{1}{2}\pi^2-\frac{1}{48}\pi^4$	$\frac{1}{16}\pi^4-\frac{1}{2}\pi^2$	$-\frac{1}{12}\pi^4$	$\frac{1}{24}\pi^4$	0
CASE -B	1	1	–2	1	0	0	0
CASE -C	3	1	–4	4	0	0	0
CASE -D	2	0	–1	2	0	0	0
CASE -E	1	0	2	–1	0	0	0

The differential Eq. (9) can be solved exactly by the power series solution, using Frobenius method:

$$Y_m = \sum_{n=0}^{\infty} C_{m,n}\eta^n. \tag{10}$$

By substituting the power series of Eq. (10) in (9), the result is as follows:

$$\begin{aligned}
&D_{22}\left(\frac{1}{b}\right)^4\left(\sum_{n=4}^{\infty} n(n-1)(n-2)(n-3)C_{m,n}\eta^{n-4}\right)\\
&\quad+\left[-2(D_{12}+2D_{66})\left(\frac{m\pi}{ab}\right)^2 - K_s\left(\frac{1}{b^2}\right)\right.\\
&\quad\left.+\left(\frac{R}{b^2}\right)\mu N_0\left(a_0+\frac{a_1}{2}+\frac{a_2}{3}+\frac{a_3}{4}+\frac{a_4}{5}+\frac{a_5}{6}\right)\right]\\
&\quad\left(\sum_{n=2}^{\infty} n(n-1)C_{m,n}\eta^{n-2}\right)\\
&\quad+\left[D_{11}\left(\frac{m\pi}{a}\right)^4 + K_w + K_s\left(\frac{m\pi}{a}\right)^2 - \mu N_0\left(a_0+a_1\eta+a_2\eta^2+a_3\eta^3+a_4\eta^4+a_5\eta^5\right)\left(\frac{m\pi}{a}\right)^2\right]\left(\sum_{n=0}^{\infty} C_{m,n}\eta^n\right) = 0
\end{aligned} \tag{11}$$

By collecting the indexes of Eq. (11), multiplying two equal sides of the equation in b^4/D_1, and considering the following dimensionless parameters, Eq. (12) results as follows:

$$\begin{aligned}
&D_{11} = D_1, \quad D_{22} = D_2, \quad (D_{12}+2D_{66}) = D_3\\
&Q = \frac{a}{b}, \quad \bar{K}_w = \frac{K_w b^4}{D_1}, \quad \bar{K}_s = \frac{K_s b^2}{D_1}, \quad N_0 = \frac{N_0 b^2}{D_1}, \quad \beta = \frac{m\pi}{Q}.
\end{aligned} \tag{12}$$

After rearranging, Eq. (13) is obtained in the following way:

$$\begin{aligned}
&\sum_{n=0}^{\infty}\left(\left(\frac{D_2}{D_1}(n+4)(n+3)(n+2)(n+1)C_{m,n+4} + \left[-2\frac{D_3}{D_1}(\beta)^2 - \bar{K}_s + \left(a_0+\frac{a_1}{2}+\frac{a_2}{3}+\frac{a_3}{4}+\frac{a_4}{5}+\frac{a_5}{6}\right)\mu R\bar{N}_0\right]\right.\right.\\
&\quad\left.\times (n+2)(n+1)C_{m,n+2} + \left[(\beta)^4 + \bar{K}_w + \bar{K}_s(\beta)^2 - a_0\mu\bar{N}_0(\beta)^2\right]C_{m,n}\right)\eta^n\\
&\quad-\left(a_1\mu\bar{N}_0(\beta)^2C_{m,n}\right)\eta^{n+1} - \left(a_2\mu\bar{N}_0(\beta)^2C_{m,n}\right)\eta^{n+2} - \left(a_3\mu\bar{N}_0(\beta)^2C_{m,n}\right)\eta^{n+3}\\
&\quad\left.-\left(a_4\mu\bar{N}_0(\beta)^2C_{m,n}\right)\eta^{n+4} - \left(a_5\mu\bar{N}_0(\beta)^2C_{m,n}\right)\eta^{n+5}\right) = 0.
\end{aligned} \tag{13}$$

According to the same indexes for coefficient η^0, the following equation is obtained:

$$C_{m,4}=\left(\frac{D_1}{24D_2}\right)\left(-2\left[-2\frac{D_3}{D_1}(\beta)^2-\bar{K}_s+\left(a_0+\frac{a_1}{2}+\frac{a_2}{3}+\frac{a_3}{4}+\frac{a_4}{5}+\frac{a_5}{6}\right)R\mu\bar{N}_0\right]C_{m,2}\right.$$
$$\left.-\left[(\beta)^4+\bar{K}_w+\bar{K}_s(\beta)^2-a_0\mu\bar{N}_0(\beta)^2\right]C_{m,0}\right) \tag{14}$$

and for coefficient η^1, it can be calculated that:

$$C_{m,5}=\left(\frac{D_1}{120D_2}\right)\left(-6\left[-2\frac{D_3}{D_1}(\beta)^2-\bar{K}_s+\left(a_0+\frac{a_1}{2}+\frac{a_2}{3}+\frac{a_3}{4}+\frac{a_4}{5}+\frac{a_5}{6}\right)R\mu\bar{N}_0\right]C_{m,3}\right.$$
$$\left.-\left[(\beta)^4+\bar{K}_w+\bar{K}_s(\beta)^2-a_0\mu\bar{N}_0(\beta)^2\right]C_{m,1}+\left(a_1\mu\bar{N}_0(\beta)^2C_{m,0}\right)\right) \tag{15}$$

and for coefficient η^2,

$$C_{m,6}=\left(\frac{D_1}{360D_2}\right)\left(-12\left[-2\frac{D_3}{D_1}(\beta)^2-\bar{K}_s+\left(a_0+\frac{a_1}{2}+\frac{a_2}{3}+\frac{a_3}{4}+\frac{a_4}{5}+\frac{a_5}{6}\right)R\mu\bar{N}_0\right]C_{m,4}\right.$$
$$\left.-\left[(\beta)^4+\bar{K}_w+\bar{K}_s(\beta)^2-a_0\mu\bar{N}_0(\beta)^2\right]C_{m,2}+\left(a_1\mu\bar{N}_0(\beta)^2C_{m,1}\right)+\left(a_2\mu\bar{N}_0(\beta)^2C_{m,0}\right)\right) \tag{16}$$

and for the coefficient η^3,

$$C_{m,7}=\left(\frac{D_1}{840D_2}\right)\left(-20\left[-2\frac{D_3}{D_1}(\beta)^2-\bar{K}_s+\left(a_0+\frac{a_1}{2}+\frac{a_2}{3}+\frac{a_3}{4}+\frac{a_4}{5}+\frac{a_5}{6}\right)R\mu\bar{N}_0\right]C_{m,5}\right.$$
$$-\left[(\beta)^4+\bar{K}_w+\bar{K}_s(\beta)^2-a_0\mu\bar{N}_0(\beta)^2\right]C_{m,3}+\left(a_1\mu\bar{N}_0(\beta)^2C_{m,2}\right)$$
$$\left.+\left(a_2\mu\bar{N}_0(\beta)^2C_{m,1}\right)+\left(a_3\mu\bar{N}_0(\beta)^2C_{m,0}\right)\right) \tag{17}$$

and for coefficient η^4,

$$C_{m,8}=\left(\frac{D_1}{1680D_2}\right)\left(-30\left[-2\frac{D_3}{D_1}(\beta)^2-\bar{K}_s+\left(a_0+\frac{a_1}{2}+\frac{a_2}{3}+\frac{a_3}{4}+\frac{a_4}{5}+\frac{a_5}{6}\right)R\mu\bar{N}_0\right]C_{m,6}\right.$$
$$-\left[(\beta)^4+\bar{K}_w+\bar{K}_s(\beta)^2-a_0\mu\bar{N}_0(\beta)^2\right]C_{m,4}+\left(a_1\mu\bar{N}_0(\beta)^2C_{m,3}\right)$$
$$\left.+\left(a_2\mu\bar{N}_0(\beta)^2C_{m,2}\right)+\left(a_3\mu\bar{N}_0(\beta)^2C_{m,1}\right)+\left(a_4\mu\bar{N}_0(\beta)^2C_{m,0}\right)\right) \tag{18}$$

and for η^n $\eta=5, 6, 7, \ldots$ equals:

$$C_{m,n+4}=\frac{D_1}{D_2(n+4)(n+3)(n+2)(n+1)}$$
$$\left(-\left[-2\frac{D_3}{D_1}(\beta)^2-\bar{K}_s\right.\right.$$
$$\left.+\left(a_0+\frac{a_1}{2}+\frac{a_2}{3}+\frac{a_3}{4}+\frac{a_4}{5}+\frac{a_5}{6}\right)R\mu\bar{N}_0\right](n+2)(n+1)C_{m,n+2}$$
$$-\left[(\beta)^4+\bar{K}_w+\bar{K}_s(\beta)^2-a_0\mu\bar{N}_0(\beta)^2\right]C_{m,n}+a_1\mu\bar{N}_0(\beta)^2C_{m,n-1}+a_2\mu\bar{N}_0(\beta)^2C_{m,n-2}$$
$$\left.+a_3\mu\bar{N}_0(\beta)^2C_{m,n-3}+a_4\mu\bar{N}_0(\beta)^2C_{m,n-4}+a_5\mu\bar{N}_0(\beta)^2C_{m,n-5}\right) \tag{19}$$

Table 2 Convergence test of the critical buckling load factors for orthotropic rectangular thin plate under biaxial non-uniform in-plane loading resting on Pasternak elastic foundation for CASE-A

Boundary conditions	N					
	20	30	40	45	50	55
SCSC	45.923$^{(1)}$	44.617$^{(2)}$	**44.831$^{(2)}$**	44.831$^{(2)}$	44.831$^{(2)}$	44.831$^{(2)}$
SSSC	32.934$^{(1)}$	**33.102$^{(1)}$**	33.102$^{(1)}$	33.102$^{(1)}$	33.102$^{(1)}$	33.102$^{(1)}$
SSSS	26.695$^{(1)}$	26.473$^{(1)}$	**26.474$^{(1)}$**	26.474$^{(1)}$	26.474$^{(1)}$	26.474$^{(1)}$
SSSF	25.717$^{(1)}$	24.982$^{(1)}$	**24.983$^{(1)}$**	24.983$^{(1)}$	24.983$^{(1)}$	24.983$^{(1)}$

$Q = 2$, $R = 1$, $\bar{K}_w, \bar{K}_s = 10$, $E_x/E_y = 2$

Equations (14)–(19) are reversibility equations for $C_{m,n}$ as arbitrary coefficients when $n \geq 4$.

2.3 Types of loading

Once the rectangular plate is subjected to in-plane CASE-A loading according to Fig. 2, $-N_0$ (load factor per length unit) is the intensity of compressing force in $\eta = 1/2$. Based on Eq. (20) to solve this state, Cosine Taylor polynomial expansion is used.

$$N_x = -N_0 \cos\pi\left(\eta - \frac{1}{2}\right) \tag{20}$$

and,

$$N_x = -N_0 \cos\pi\left(\eta - \frac{1}{2}\right) = -N_0 \sum_{n=0}^{\infty} \frac{(-1)^n \left(\pi\left(\eta - \frac{1}{2}\right)\right)^{2n}}{(2n)!}. \tag{20-a}$$

By expanding and arranging the abovementioned series, and as regards the sum of the first three terms has sufficient accuracy:

$$N_x = -N_0\left(1 - \frac{1}{2}\pi^2\left(\eta - \frac{1}{2}\right)^2 + \frac{1}{24}\pi^4\left(\eta - \frac{1}{2}\right)^4\right) \tag{20-b}$$

and,

$$N_x = -N_0\left(\frac{1}{24}\pi^4\eta^4 - \frac{1}{12}\pi^4\eta^3 + \left(\frac{1}{16}\pi^4 - \frac{1}{2}\pi^2\right)\eta^2 + \left(\frac{1}{2}\pi^2 - \frac{1}{48}\pi^4\right)\eta + \left(1 - \frac{1}{8}\pi^2 + \frac{1}{384}\pi^4\right)\right). \tag{21}$$

By naming the terms like Table 1 as follows, the values of a_i are obtained:

$$\begin{aligned} a_0 &= 1 - \frac{1}{8}\pi^2 + \frac{1}{384}\pi^4 \\ a_1 &= \frac{1}{2}\pi^2 - \frac{1}{48}\pi^4 \\ a_2 &= \frac{1}{16}\pi^4 - \frac{1}{2}\pi^2 \\ a_3 &= -\frac{1}{12}\pi^4 \quad a_4 = \frac{1}{24}\pi^4, \quad a_5 = 0. \end{aligned} \tag{22}$$

Generally, for the other kinds of loadings of A, B, C, D, and E, the values of a_i and μ can be replaced in Eq. (9) and can be solved by Frobenius method.

3 Boundary conditions

So far, different values of $C_{m,n}$ are obtained by reversible relationships in terms of $C_{m,0}$, $C_{m,1}$, $C_{m,2}$, and $C_{m,3}$. To calculate the values of these coefficients, it is required to have the equations that can be achieved by applying the boundary conditions. For each edge of the plate $\eta = 0$, 1 according to the boundary conditions, two equations can be written. These two edges may admit any boundary condition (including simply, clamped, and free-edged support). For dimensionless boundary conditions, we give:

$$\begin{aligned} &\text{Simply} \quad w = 0, \quad \frac{\partial w}{\partial \eta} = 0 \\ &\text{Clamped} \quad w = 0, \quad \frac{\partial w}{\partial \eta} = 0 \\ &\text{Free} \quad \frac{\partial^2 w}{\partial \eta^2} + \nu\frac{\partial^2 w}{\partial \xi^2} = 0, \\ &\quad \frac{\partial^3 w}{\partial \eta^3} + (2-\nu)\frac{\partial^3 w}{\partial \eta \partial \xi^2} + \bar{K}_s\frac{\partial w}{\partial \eta} = 0. \end{aligned} \tag{23}$$

By substituting Eq. (5) in (23), the following equations can be obtained:

$$\begin{aligned} &\text{Simply} \quad Y_m = 0, Y_m'' = 0 \\ &\text{Clamped} \quad Y_m = 0, Y_m' = 0 \\ &\text{Free} \quad Y_m'' - \nu\left(\frac{m\pi}{Q}\right)^2 Y_m = 0, \\ &\quad Y_m''' - \left[(2-\nu)\left(\frac{m\pi}{Q}\right)^2 + \bar{K}_s\right]Y_m' = 0. \end{aligned} \tag{24}$$

Table 3 Comparison of the critical buckling load parameter ($\bar{N}_{cr}$) for a thin square plate ($Q = 1$) subjected to uniformly and linearly distributed in-plane compressive loading resting on Pasternak elastic foundation

$(\bar{K}_w, \bar{K}_s)$	α	References	Boundary conditions			
			SCSC	SSSC	SSSS	SSSF
(10, 100)	0.5	Bodaghi and Saidi [30] present study	270.562$^{(2)}$	251.325$^{(2)}$	245.480$^{(2)}$	215.029$^{(1)}$
			270.562$^{(2)}$	251.325$^{(2)}$	245.480$^{(2)}$	215.028$^{(1)}$
(100, 10)	0	Akhavan et al. [27] present study	91.363$^{(2)}$	82.902$^{(2)}$	69.610$^{(1)}$	–
			91.365$^{(2)}$	82.903$^{(2)}$	69.610$^{(1)}$	36.801$^{(1)}$
(1000, 100)	0	Akhavan et al. [27] present study	229.971$^{(2)}$	219.968$^{(2)}$	212.014$^{(2)}$	–
			229.973$^{(2)}$	219.969$^{(2)}$	212.015$^{(2)}$	175.260$^{(1)}$

$N_x = (1 - \alpha\eta)$, $E_x/E_y = 1$

4 Critical buckling load

By applying different boundary conditions to each kind of loading, four equations with variables $C_{m,0}$, $C_{m,1}$, $C_{m,2}$, and $C_{m,3}$ are achieved. To obtain a non-trivial solution of the system, the determinant of the coefficients matrix is set to zero. By solving the eigenvalue equation, the values of dimensionless buckling loads of $\bar{N}_0$ can be achieved. Substituting each $\bar{N}_0$ in four homogeneous equations, the values of corresponding eigenvectors of $C_{m,n}$ representing the shape mode (m) can be determined. The minimum value of $\bar{N}_0$ represents the critical buckling load. Numerical results of power series method are presented in the next section and are achieved according to Table 2, considering adequate term ($N = 55$) for convergence. In this table, N is the total number of existing terms in the power series solution method. The highlighted critical buckling load shows the best convergence values in each column with minimum N.

5 Evaluation of accuracy and reliability of results

To demonstrate the validity of the results of Frobenius solution for rectangular plate, first they have been compared with those in the literature review in Tables 3 and 4, and for all boundary conditions, validity and accuracy are observed.

6 The analytical results and discussion

6.1 The effect of ratio of elasticity modulus and the method of loading on the critical buckling load

To examine the critical dimensionless buckling load in each type of loading according to boundary conditions, two tables are presented. In the first table, the coefficient values of Winkler and Pasternak foundations (lateral and shear stiffness) have been fixed, and the effects of boundary conditions, aspect ratio, the ratio of modulus of elasticity, and the kind of loadings as uniaxial and biaxial are investigated. Superscript numbers in parentheses represent the buckling mode. Based on Tables 5, 6, 7, 8 and 9, it can be found that the critical buckling load generally decreases as aspect ratio (Q) increases. As a result, the maximum buckling corresponds to the aspect ratio ($Q = 0.5$). Additionally, it can be seen that by increasing the aspect ratio, the critical buckling load factor sometimes remains constant; for example, in the Table 5 for rectangular plate (CASE-A) with the boundary condition (SCSC) and ($R = 0$), when $E_x/E_y = 0.5$, the critical dimensionless buckling load $\bar{N}_{cr} = 259.352$ is obtained for aspect ratio ($Q = 0.5$, $m = 1$), ($Q = 1$, $m = 2$), and $Q = 2$, $m = 4$. This is due to the fact that parameter β appears to determine the coefficients matrix.

Table 4 Comparison of the critical buckling load parameter ($\bar{N}_{\mathrm{cr}}$) for thin rectangular plates subjected to uniformly and linearly distributed in-plane compressive loading

Boundary conditions	Q	α	Reference [4]	Reference [27]	Present study
SCSC	0.67	0	68.800$^{(1)}$	68.816$^{(1)}$	68.816$^{(1)}$
	0.66	0.5	91.430$^{(1)}$	92.415$^{(1)}$	91.429$^{(1)}$
SSSC	0. 8	0	53.390$^{(1)}$	53.393$^{(1)}$	53.393$^{(1)}$
	0.78	0.5	68.480$^{(1)}$	68.977$^{(1)}$	68.522$^{(1)}$
SSSS	1	0	39.480$^{(1)}$	39.478$^{(1)}$	39.478$^{(1)}$
	1	0.5	52.490$^{(1)}$	50.673$^{(1)}$	52.494$^{(1)}$
SSSF	10	0	4.200$^{(1)}$	4.282$^{(1)}$	4.295$^{(1)}$
	10	0.5	6.700$^{(1)}$	6.765$^{(1)}$	6.871$^{(1)}$

$N_x = (1 - \alpha\eta)$, $E_x/E_y = 1$

While the ratio of coefficients of m and Q in that parameter has been chosen as a constant value, the buckling load factor does not change. It should be noted that this phenomenon is a familiar behavior in buckling of plates, that is not limited to orthotropic plates on elastic foundation. Furthermore, by increasing the aspect ratio, the critical buckling load factor remains occasionally constant, whereas the critical buckling mode increases. As it is evident in all tables, the maximum buckling mode corresponds to the aspect ratio $Q = 10$.

Table 5 The critical buckling load factor ($\bar{N}_{cr}$) for the isotropic and orthotropic rectangular plate with different boundary conditions under axial and biaxial non-uniform in-plane loading for CASE-A

$\frac{E_x}{E_y}$	Boundary conditions	Q							
		0.5		1		2		10	
		R							
		0	1	0	1	0	1	0	1
0.5	SCSC	$259.352^{(1)}$	$212.744^{(1)}$	$259.352^{(2)}$	$212.744^{(2)}$	$259.352^{(4)}$	$209.274^{(3)}$	$257.272^{(22)}$	$208.731^{(16)}$
	SSSC	$245.150^{(1)}$	$203.632^{(1)}$	$245.150^{(2)}$	$197.447^{(1)}$	$245.150^{(4)}$	$193.892^{(3)}$	$245.060^{(21)}$	$193.384^{(14)}$
	SSSS	$233.236^{(1)}$	$196.267^{(1)}$	$233.236^{(2)}$	$179.433^{(1)}$	$233.236^{(4)}$	$179.433^{(2)}$	$232.984^{(19)}$	$178.968^{(11)}$
	SSSF	$215.384^{(1)}$	$193.149^{(1)}$	$215.384^{(2)}$	$172.325^{(1)}$	$208.009^{(3)}$	$172.325^{(2)}$	$208.009^{(15)}$	$172.150^{(11)}$
1	SCSC	$233.782^{(1)}$	$191.769^{(1)}$	$233.782^{(2)}$	$188.636^{(1)}$	$233.782^{(4)}$	$183.088^{(3)}$	$233.578^{(21)}$	$182.882^{(14)}$
	SSSC	$226.536^{(1)}$	$188.054^{(1)}$	$226.536^{(2)}$	$176.146^{(1)}$	$226.536^{(4)}$	$176.146^{(2)}$	$226.536^{(20)}$	$174.584^{(12)}$
	SSSS	$220.103^{(1)}$	$184.811^{(1)}$	$220.103^{(2)}$	$167.091^{(1)}$	$220.103^{(4)}$	$167.091^{(2)}$	$219.579^{(20)}$	$166.843^{(11)}$
	SSSF	$208.335^{(1)}$	$183.772^{(1)}$	$208.335^{(2)}$	$163.709^{(1)}$	$201.970^{(3)}$	$163.709^{(2)}$	$201.950^{(16)}$	$163.645^{(11)}$
2	SCSC	$219.123^{(1)}$	$179.152^{(1)}$	$219.123^{(2)}$	$169.472^{(1)}$	$219.123^{(4)}$	$168.237^{(3)}$	$219.123^{(20)}$	$167.025^{(13)}$
	SSSC	$214.817^{(1)}$	$177.831^{(1)}$	$214.817^{(2)}$	$163.962^{(1)}$	$214.817^{(4)}$	$163.962^{(2)}$	$214.641^{(19)}$	$163.039^{(12)}$
	SSSS	$211.348^{(1)}$	$176.598^{(1)}$	$211.348^{(2)}$	$159.536^{(1)}$	$211.348^{(4)}$	$159.536^{(2)}$	$210.655^{(19)}$	$159.260^{(11)}$
	SSSF	$205.320^{(1)}$	$176.330^{(1)}$	$205.320^{(2)}$	$157.918^{(1)}$	$199.851^{(3)}$	$157.918^{(2)}$	$199.358^{(16)}$	$157.777^{(11)}$
3	SCSC	$214.581^{(1)}$	$174.056^{(1)}$	$214.581^{(2)}$	$162.603^{(1)}$	$214.581^{(4)}$	$162.598^{(3)}$	$213.321^{(21)}$	$160.960^{(12)}$
	SSSC	$212.798^{(1)}$	$173.401^{(1)}$	$212.798^{(2)}$	$159.274^{(1)}$	$212.798^{(4)}$	$159.274^{(2)}$	$212.328^{(18)}$	$158.475^{(12)}$
	SSSS	$210.403^{(1)}$	$172.771^{(1)}$	$210.403^{(2)}$	$156.430^{(1)}$	$210.403^{(4)}$	$156.430^{(2)}$	$209.626^{(18)}$	$156.086^{(11)}$
	SSSF	$202.827^{(1)}$	$172.694^{(1)}$	$202.827^{(2)}$	$155.480^{(1)}$	$198.124^{(3)}$	$155.480^{(2)}$	$197.631^{(16)}$	$155.239^{(11)}$

$\bar{K}_w = 100, \bar{K}_s = 100$

Table 6 The critical buckling load factor ($\bar{N}_{cr}$) for the isotropic and orthotropic rectangular plate with different boundary conditions under axial and biaxial non-uniform in-plane loading for CASE-B

$\frac{E_x}{E_y}$	Boundary conditions	Q							
		0.5		1		2		10	
		R							
		0	1	0	1	0	1	0	1
0.5	SCSC	$364.568^{(1)}$	$275.596^{(1)}$	$364.568^{(2)}$	$242.359^{(1)}$	$364.568^{(4)}$	$242.359^{(2)}$	$364.568^{(20)}$	$241.529^{(11)}$
	SSSC	$261.433^{(1)}$	$204.077^{(1)}$	$261.433^{(2)}$	$150.175^{(1)}$	$252.549^{(3)}$	$148.753^{(1)}$	$251.018^{(16)}$	$147.402^{(7)}$
	SSSS	$253.981^{(1)}$	$200.416^{(1)}$	$253.981^{(2)}$	$124.552^{(1)}$	$232.631^{(3)}$	$100.898^{(1)}$	$232.226^{(14)}$	$92.612^{(1)}$
	SSSF	$247.452^{(1)}$	$200.348^{(1)}$	$197.059^{(1)}$	$123.593^{(1)}$	$197.059^{(2)}$	$102.493^{(1)}$	$197.059^{(10)}$	$100.920^{(3)}$
1	SCSC	$279.394^{(1)}$	$211.349^{(1)}$	$279.394^{(2)}$	$154.811^{(1)}$	$278.903^{(3)}$	$149.440^{(1)}$	$273.478^{(17)}$	$149.440^{(5)}$
	SSSC	$213.990^{(1)}$	$165.382^{(1)}$	$213.990^{(2)}$	$105.116^{(1)}$	$194.235^{(3)}$	$94.258^{(1)}$	$194.079^{(14)}$	$93.048^{(1)}$
	SSSS	$211.605^{(1)}$	$164.775^{(1)}$	$194.854^{(1)}$	$94.770^{(1)}$	$186.353^{(3)}$	$71.405^{(1)}$	$183.357^{(13)}$	$63.009^{(1)}$
	SSSF	$209.677^{(1)}$	$164.849^{(1)}$	$163.867^{(1)}$	$96.006^{(1)}$	$163.867^{(2)}$	$75.245^{(1)}$	$163.867^{(10)}$	$72.149^{(2)}$
2	SCSC	$225.526^{(1)}$	$169.020^{(1)}$	$225.526^{(2)}$	$107.642^{(1)}$	$210.931^{(3)}$	$94.370^{(1)}$	$210.931^{(15)}$	$91.583^{(1)}$
	SSSC	$181.980^{(1)}$	$137.911^{(1)}$	$167.470^{(1)}$	$79.535^{(1)}$	$158.226^{(3)}$	$65.942^{(1)}$	$155.644^{(13)}$	$62.855^{(1)}$
	SSSS	$181.329^{(1)}$	$137.885^{(1)}$	$156.013^{(1)}$	$76.249^{(1)}$	$155.373^{(3)}$	$55.559^{(1)}$	$150.323^{(12)}$	$48.156^{(1)}$
	SSSF	$180.896^{(1)}$	$137.870^{(1)}$	$142.333^{(1)}$	$77.007^{(1)}$	$142.333^{(2)}$	$58.754^{(1)}$	$142.194^{(11)}$	$55.785^{(2)}$
3	SCSC	$202.766^{(1)}$	$150.186^{(1)}$	$202.766^{(2)}$	$90.485^{(1)}$	$184.290^{(3)}$	$75.587^{(1)}$	$184.187^{(14)}$	$71.885^{(1)}$
	SSSC	$167.814^{(1)}$	$125.073^{(1)}$	$147.315^{(1)}$	$69.703^{(1)}$	$143.411^{(3)}$	$56.086^{(1)}$	$139.621^{(13)}$	$52.769^{(1)}$
	SSSS	$167.531^{(1)}$	$125.073^{(1)}$	$140.284^{(1)}$	$68.368^{(1)}$	$140.284^{(2)}$	$49.835^{(1)}$	$136.058^{(12)}$	$43.187^{(1)}$
	SSSF	$167.374^{(1)}$	$125.057^{(1)}$	$132.303^{(1)}$	$68.686^{(1)}$	$132.303^{(2)}$	$52.376^{(1)}$	$131.619^{(11)}$	$49.623^{(2)}$

$\bar{K}_w = 10, \bar{K}_s = 10$

Table 7 The critical buckling load factor ($\bar{N}_{cr}$) for the isotropic and orthotropic rectangular plate with different boundary conditions under axial and biaxial non-uniform in-plane loading for CASE-C

$\frac{E_x}{E_y}$	Boundary conditions	Q							
		0.5		1		2		10	
		R							
		0	1	0	1	0	1	0	1
0.5	SCSC	$335.628^{(1)}$	$189.199^{(1)}$	$335.628^{(2)}$	$111.824^{(1)}$	$335.628^{(4)}$	$94.741^{(1)}$	$332.820^{(22)}$	$89.909^{(1)}$
	SSSC	$212.505^{(1)}$	$125.405^{(1)}$	$212.505^{(2)}$	$71.904^{(1)}$	$212.505^{(4)}$	$56.271^{(1)}$	$210.669^{(18)}$	$51.405^{(1)}$
	SSSS	$183.829^{(1)}$	$118.980^{(1)}$	$183.829^{(2)}$	$56.081^{(1)}$	$170.396^{(3)}$	$37.189^{(1)}$	$170.259^{(14)}$	$31.011^{(1)}$
	SSSF	$48.006^{(1)}$	$53.211^{(1)}$	$30.991^{(1)}$	$36.561^{(1)}$	$30.991^{(2)}$	$36.560^{(2)}$	$30.742^{(9)}$	$36.324^{(9)}$
1	SCSC	$246.508^{(1)}$	$137.399^{(1)}$	$246.508^{(2)}$	$71.710^{(1)}$	$246.508^{(4)}$	$55.025^{(1)}$	$246.382^{(19)}$	$50.420^{(1)}$
	SSSC	$165.232^{(1)}$	$94.537^{(1)}$	$165.232^{(2)}$	$50.120^{(1)}$	$160.693^{(3)}$	$35.651^{(1)}$	$160.111^{(16)}$	$31.196^{(1)}$
	SSSS	$150.021^{(1)}$	$93.924^{(1)}$	$142.836^{(1)}$	$43.033^{(1)}$	$135.483^{(3)}$	$26.339^{(1)}$	$133.983^{(13)}$	$21.097^{(1)}$
	SSSF	$36.441^{(1)}$	$40.672^{(1)}$	$22.105^{(1)}$	$27.351^{(1)}$	$22.105^{(2)}$	$27.351^{(2)}$	$21.701^{(9)}$	$27.351^{(10)}$
2	SCSC	$239.069^{(1)}$	$95.548^{(1)}$	$239.069^{(2)}$	$50.229^{(1)}$	$188.824^{(3)}$	$34.760^{(1)}$	$186.004^{(17)}$	$30.658^{(1)}$
	SSSC	$132.012^{(1)}$	$71.981^{(1)}$	$132.012^{(2)}$	$37.460^{(1)}$	$125.168^{(3)}$	$24.932^{(1)}$	$125.168^{(15)}$	$21.073^{(1)}$
	SSSS	$124.250^{(1)}$	$70.351^{(1)}$	$113.811^{(1)}$	$35.111^{(1)}$	$111.109^{(3)}$	$20.525^{(1)}$	$108.893^{(13)}$	$16.124^{(1)}$
	SSSF	$32.077^{(1)}$	$34.054^{(1)}$	$18.036^{(1)}$	$20.853^{(1)}$	$18.036^{(2)}$	$20.853^{(2)}$	$17.168^{(8)}$	$20.745^{(9)}$
3	SCSC	$195.026^{(1)}$	$79.814^{(1)}$	$195.026^{(1)}$	$42.526^{(1)}$	$160.443^{(3)}$	$27.851^{(1)}$	$160.443^{(15)}$	$24.063^{(1)}$
	SSSC	$116.694^{(1)}$	$61.961^{(1)}$	$116.694^{(2)}$	$32.282^{(1)}$	$110.011^{(3)}$	$21.195^{(1)}$	$110.011^{(15)}$	$17.691^{(1)}$
	SSSS	$109.751^{(1)}$	$60.784^{(1)}$	$101.723^{(1)}$	$31.799^{(1)}$	$99.991^{(3)}$	$18.440^{(1)}$	$97.816^{(13)}$	$23.502^{(1)}$
	SSSF	$29.935^{(1)}$	$31.368^{(1)}$	$16.217^{(1)}$	$18.364^{(1)}$	$16.217^{(2)}$	$18.364^{(2)}$	$15.192^{(7)}$	$18.108^{(9)}$

$\bar{K}_w = 10, \bar{K}_s = 10$

Table 8 The critical buckling load factor ($\bar{N}_{cr}$) for the isotropic and orthotropic rectangular plate with different boundary conditions under axial and biaxial nonlinear in-plane loading for CASE-D

$\frac{E_x}{E_y}$	Boundary conditions	Q							
		0.5		1		2		10	
		R							
		0	1	0	1	0	1	0	1
0.5	SCSC	$418.114^{(1)}$	$308.224^{(1)}$	$418.114^{(2)}$	$300.742^{(1)}$	$393.217^{(5)}$	$282.029^{(1)}$	$392.347^{(26)}$	$269.725^{(1)}$
	SSSC	$417.144^{(1)}$	$308.147^{(1)}$	$417.144^{(2)}$	$276.104^{(1)}$	$393.025^{(5)}$	$186.272^{(1)}$	$392.210^{(26)}$	$154.860^{(1)}$
	SSSS	$240.929^{(1)}$	$188.995^{(1)}$	$240.929^{(2)}$	$144.592^{(1)}$	$240.929^{(4)}$	$110.402^{(1)}$	$240.273^{(19)}$	$93.031^{(1)}$
	SSSF	$62.926^{(1)}$	$65.277^{(1)}$	$40.799^{(1)}$	$42.963^{(1)}$	$40.799^{(2)}$	$42.963^{(2)}$	$40.551^{(9)}$	$42.669^{(9)}$
1	SCSC	$291.136^{(1)}$	$215.692^{(1)}$	$291.136^{(2)}$	$215.690^{(1)}$	$288.918^{(5)}$	$163.571^{(1)}$	$287.038^{(23)}$	$151.258^{(1)}$
	SSSC	$290.941^{(1)}$	$215.683^{(1)}$	$290.941^{(2)}$	$182.257^{(1)}$	$288.891^{(5)}$	$118.069^{(1)}$	$286.979^{(23)}$	$93.980^{(1)}$
	SSSS	$185.569^{(1)}$	$144.395^{(1)}$	$185.569^{(2)}$	$104.382^{(1)}$	$183.482^{(3)}$	$77.815^{(1)}$	$181.729^{(17)}$	$63.294^{(1)}$
	SSSF	$48.674^{(1)}$	$50.711^{(1)}$	$29.203^{(1)}$	$31.030^{(1)}$	$29.203^{(2)}$	$31.030^{(1)}$	$28.680^{(9)}$	$30.523^{(9)}$
2	SCSC	$213.729^{(1)}$	$158.083^{(1)}$	$213.729^{(2)}$	$124.810^{(1)}$	$213.729^{(4)}$	$103.041^{(1)}$	$213.729^{(20)}$	$91.972^{(1)}$
	SSSC	$213.697^{(1)}$	$158.062^{(1)}$	$213.697^{(2)}$	$124.612^{(1)}$	$213.697^{(4)}$	$82.654^{(1)}$	$213.697^{(20)}$	$63.486^{(1)}$
	SSSS	$148.300^{(1)}$	$113.884^{(1)}$	$148.300^{(2)}$	$78.477^{(1)}$	$141.518^{(3)}$	$60.039^{(1)}$	$141.508^{(16)}$	$48.374^{(1)}$
	SSSF	$43.453^{(1)}$	$44.361^{(1)}$	$24.025^{(1)}$	$24.891^{(1)}$	$24.025^{(2)}$	$24.891^{(2)}$	$22.848^{(8)}$	$23.746^{(8)}$
3	SCSC	$182.449^{(1)}$	$134.411^{(1)}$	$182.449^{(2)}$	$101.375^{(1)}$	$182.449^{(4)}$	$82.324^{(1)}$	$181.867^{(19)}$	$72.189^{(1)}$
	SSSC	$182.438^{(1)}$	$134.400^{(1)}$	$182.438^{(2)}$	$101.357^{(1)}$	$182.438^{(4)}$	$70.346^{(1)}$	$181.849^{(19)}$	$53.300^{(1)}$
	SSSS	$132.153^{(1)}$	$100.478^{(1)}$	$132.153^{(2)}$	$67.556^{(1)}$	$124.006^{(3)}$	$53.379^{(1)}$	$124.006^{(15)}$	$43.381^{(1)}$
	SSSF	$40.947^{(1)}$	$41.563^{(1)}$	$21.774^{(1)}$	$22.395^{(1)}$	$21.774^{(2)}$	$22.395^{(2)}$	$20.350^{(7)}$	$21.027^{(7)}$

$\bar{K}_w = 10, \bar{K}_s = 10$

Table 9 The critical buckling load factor ($\bar{N}_{cr}$) for the isotropic and orthotropic rectangular plate with different boundary conditions under axial and biaxial non-uniform in-plane loading for CASE-E

$\frac{E_x}{E_y}$	Boundary conditions	Q							
		0.5		1		2		10	
		R							
		0	1	0	1	0	1	0	1
0.5	SCSC	308.898$^{(1)}$	242.914$^{(1)}$	308.898$^{(2)}$	242.461$^{(1)}$	307.489$^{(5)}$	235.256$^{(3)}$	305.157$^{(23)}$	235.256$^{(15)}$
	SSSC	299.009$^{(1)}$	238.610$^{(1)}$	299.009$^{(2)}$	220.453$^{(1)}$	299.009$^{(4)}$	220.453$^{(2)}$	297.941$^{(22)}$	220.348$^{(9)}$
	SSSS	265.924$^{(1)}$	214.364$^{(1)}$	265.924$^{(2)}$	190.637$^{(1)}$	265.924$^{(4)}$	190.637$^{(2)}$	265.924$^{(20)}$	190.123$^{(8)}$
	SSSF	183.769$^{(1)}$	181.671$^{(1)}$	183.769$^{(2)}$	165.240$^{(1)}$	174.407$^{(3)}$	165.240$^{(2)}$	174.407$^{(15)}$	164.211$^{(12)}$
1	SCSC	275.368$^{(1)}$	215.999$^{(1)}$	275.368$^{(2)}$	203.079$^{(1)}$	275.368$^{(4)}$	203.079$^{(2)}$	274.509$^{(21)}$	202.031$^{(12)}$
	SSSC	271.159$^{(1)}$	215.173$^{(1)}$	271.159$^{(2)}$	195.397$^{(1)}$	271.159$^{(4)}$	193.601$^{(1)}$	270.964$^{(21)}$	192.523$^{(1)}$
	SSSS	249.095$^{(1)}$	198.387$^{(1)}$	249.095$^{(2)}$	176.027$^{(1)}$	249.095$^{(4)}$	176.027$^{(2)}$	249.086$^{(19)}$	175.687$^{(8)}$
	SSSF	168.770$^{(1)}$	169.628$^{(1)}$	168.770$^{(2)}$	153.947$^{(1)}$	159.282$^{(3)}$	153.947$^{(2)}$	159.092$^{(14)}$	152.875$^{(12)}$
2	SCSC	254.441$^{(1)}$	198.066$^{(1)}$	254.441$^{(2)}$	181.306$^{(1)}$	254.441$^{(4)}$	181.306$^{(2)}$	254.330$^{(21)}$	181.268$^{(11)}$
	SSSC	252.592$^{(1)}$	198.001$^{(1)}$	252.592$^{(2)}$	179.556$^{(1)}$	252.592$^{(4)}$	178.988$^{(1)}$	252.592$^{(20)}$	177.181$^{(1)}$
	SSSS	237.605$^{(1)}$	186.250$^{(1)}$	237.605$^{(2)}$	166.069$^{(1)}$	237.605$^{(4)}$	166.069$^{(2)}$	237.529$^{(19)}$	166.022$^{(9)}$
	SSSF	161.718$^{(1)}$	160.149$^{(1)}$	159.036$^{(1)}$	144.636$^{(1)}$	151.324$^{(3)}$	144.636$^{(2)}$	150.826$^{(14)}$	143.582$^{(12)}$
3	SCSC	245.825$^{(1)}$	190.065$^{(1)}$	245.825$^{(2)}$	173.028$^{(1)}$	245.825$^{(4)}$	173.028$^{(2)}$	245.825$^{(20)}$	173.028$^{(10)}$
	SSSC	244.651$^{(1)}$	190.059$^{(1)}$	244.651$^{(2)}$	172.519$^{(1)}$	244.651$^{(4)}$	172.519$^{(2)}$	244.651$^{(20)}$	172.519$^{(10)}$
	SSSS	232.631$^{(1)}$	180.513$^{(1)}$	232.631$^{(2)}$	161.597$^{(1)}$	232.631$^{(4)}$	161.597$^{(2)}$	232.558$^{(19)}$	161.597$^{(10)}$
	SSSF	159.487$^{(1)}$	156.916$^{(1)}$	154.944$^{(1)}$	141.060$^{(1)}$	148.592$^{(3)}$	141.060$^{(2)}$	147.929$^{(14)}$	140.145$^{(12)}$

$\bar{K}_w = 100, \bar{K}_s = 100$

When the plate is subjected to uniaxial loading ($R = 0$), the critical buckling load occurs in higher modes, compared to biaxial loading. Critical buckling load values of the plate, while it is subjected to biaxial loading (there are a few exceptions), decrease in comparison with the uniaxial state. For example, in Table 7 for rectangular plate under sample loading (C) with the boundary condition SSSS when the ratio of modulus of elasticity in two different directions is 2 and the aspect ratio is $Q = 2$, the critical buckling load is reduced from the value of $\bar{N}_{cr} = 111.109$ to $\bar{N}_{cr} = 20.525$.

It can also be observed that as the ratio of the modulus of elasticity in two different directions (isotropic and orthotropic) increases, the value of dimensionless buckling load decreases. In all Tables of 5, 6, 7, 8, and 9, the maximum buckling load is associated to the plate with SCSC boundary condition. In other words, when two edges of the plate are clamped, the critical buckling load increases, compared to the simply-supported and free edges. It can also be seen in the state of uniaxial loading ($R = 0$) that the minimum buckling load is associated with SSSF plate.

6.2 The influence of stiffness coefficients of elastic foundation and combinations of boundary conditions on the critical buckling load

In this section, the influences of elastic foundation coefficients and boundary conditions for a rectangular orthotropic plate on the state of biaxial loading can be observed. According to Tables 10 and 11, it is obvious that the minimum buckling load is associated to the state in which there is a rectangular plate without elastic foundation. When $\bar{K}_W = 100, \bar{K}_S = 0$, the value of buckling load increases in comparison with that of the foundationless state. As expected, when the coefficients of elastic foundation increase, the values of dimensionless critical buckling load rise, and, rising rates of these amounts for the coefficient Pasternak elastic foundation (shear stiffness coefficient) are more than those with the variation of the coefficient of Winkler elastic foundation (lateral stiffness coefficient).

Table 10 The critical buckling load factor ($\bar{N}_{cr}$) for the orthotropic rectangular plate with different boundary conditions under biaxial non-uniform in-plane loading for CASE-A versus foundation stiffness coefficients

$(\bar{K}_w, \bar{K}_s)$	Boundary conditions	Q						
		0.5	1	1.5	2	2.5	3	10
(0, 0)	SCSC	$57.632^{(1)}$	$30.979^{(1)}$	$29.023^{(1)}$	$29.232^{(1)}$	$29.384^{(2)}$	$29.023^{(2)}$	$29.030^{(6)}$
	SSSC	$55.435^{(1)}$	$23.796^{(1)}$	$18.780^{(1)}$	$17.291^{(1)}$	$16.683^{(1)}$	$16.381^{(1)}$	$15.833^{(1)}$
	SSSS	$53.644^{(1)}$	$38.874^{(1)}$	$36.957^{(1)}$	$34.284^{(1)}$	$33.051^{(1)}$	$32.382^{(1)}$	$31.003^{(1)}$
	SSSF	$52.982^{(1)}$	$16.609^{(1)}$	$30.874^{(1)}$	$27.896^{(1)}$	$26.512^{(1)}$	$25.756^{(1)}$	$24.183^{(1)}$
(0, 100)	SCSC	$176.887^{(1)}$	$163.578^{(1)}$	$162.897^{(2)}$	$163.578^{(2)}$	$162.445^{(3)}$	$162.897^{(4)}$	$162.445^{(12)}$
	SSSC	$175.515^{(1)}$	$157.657^{(1)}$	$159.212^{(2)}$	$157.657^{(2)}$	$157.979^{(3)}$	$157.657^{(3)}$	$157.580^{(11)}$
	SSSS	$174.235^{(1)}$	$152.858^{(1)}$	$154.626^{(1)}$	$152.858^{(2)}$	$153.308^{(2)}$	$152.858^{(3)}$	$152.850^{(9)}$
	SSSF	$173.910^{(1)}$	$149.812^{(1)}$	$149.394^{(1)}$	$149.812^{(2)}$	$148.955^{(2)}$	$149.394^{(2)}$	$148.955^{(8)}$
(100, 0)	SCSC	$59.930^{(1)}$	$36.854^{(1)}$	$37.183^{(1)}$	$36.854^{(2)}$	$36.567^{(2)}$	$36.854^{(3)}$	$36.519^{(9)}$
	SSSC	$57.818^{(1)}$	$30.089^{(1)}$	$27.570^{(1)}$	$27.426^{(1)}$	$27.562^{(1)}$	$27.570^{(2)}$	$27.425^{(5)}$
	SSSS	$56.095^{(1)}$	$26.092^{(1)}$	$22.824^{(1)}$	$22.505^{(1)}$	$22.636^{(1)}$	$22.809^{(1)}$	$22.505^{(5)}$
	SSSF	$55.593^{(1)}$	$26.137^{(1)}$	$25.389^{(1)}$	$26.137^{(2)}$	$25.054^{(2)}$	$25.389^{(2)}$	$25.054^{(8)}$
(10, 10)	SCSC	$69.805^{(1)}$	$44.831^{(1)}$	$43.999^{(1)}$	$44.831^{(2)}$	$43.872^{(2)}$	$43.999^{(2)}$	$43.872^{(8)}$
	SSSC	$67.756^{(1)}$	$37.894^{(1)}$	$33.979^{(1)}$	$33.103^{(1)}$	$32.845^{(1)}$	$32.754^{(1)}$	$32.698^{(2)}$
	SSSS	$66.042^{(1)}$	$33.385^{(1)}$	$28.056^{(1)}$	$26.474^{(1)}$	$25.836^{(1)}$	$25.524^{(1)}$	$24.983^{(1)}$
	SSSF	$65.497^{(1)}$	$31.284^{(1)}$	$25.873^{(1)}$	$24.983^{(1)}$	$25.243^{(1)}$	$25.782^{(1)}$	$24.983^{(5)}$

$R = 1$, $E_x/E_y = 2$

Table 11 The critical buckling load factor ($\bar{N}_{cr}$) for the orthotropic rectangular plate with different boundary conditions under biaxial non-uniform in-plane loading for CASE-B versus foundation stiffness coefficients

$(\bar{K}_w, \bar{K}_s)$	Boundary conditions	Q						
		0.5	1	1.5	2	2.5	3	10
(0, 0)	SCSC	$142.606^{(1)}$	$74.997^{(1)}$	$64.341^{(1)}$	$61.562^{(1)}$	$60.534^{(1)}$	$60.057^{(1)}$	$59.278^{(1)}$
	SSSC	$114.666^{(1)}$	$50.413^{(1)}$	$38.328^{(1)}$	$34.510^{(1)}$	$32.880^{(1)}$	$32.041^{(1)}$	$30.434^{(1)}$
	SSSS	$114.600^{(1)}$	$45.126^{(1)}$	$28.338^{(1)}$	$22.338^{(1)}$	$19.588^{(1)}$	$18.109^{(1)}$	$15.098^{(1)}$
	SSSF	$114.592^{(1)}$	$45.352^{(1)}$	$27.284^{(1)}$	$20.133^{(1)}$	$16.659^{(1)}$	$14.726^{(1)}$	$10.626^{(1)}$
(0, 100)	SCSC	$386.846^{(1)}$	$371.376^{(1)}$	$370.239^{(1)}$	$367.606^{(1)}$	$365.389^{(1)}$	$363.831^{(1)}$	$359.697^{(1)}$
	SSSC	$335.274^{(1)}$	$318.948^{(1)}$	$318.680^{(2)}$	$318.948^{(2)}$	$318.111^{(3)}$	$318.680^{(4)}$	$318.111^{(12)}$
	SSSS	$335.274^{(1)}$	$318.749^{(1)}$	$318.656^{(2)}$	$318.749^{(2)}$	$318.053^{(3)}$	$318.656^{(4)}$	$318.053^{(12)}$
	SSSF	$335.270^{(1)}$	$318.818^{(1)}$	$318.645^{(2)}$	$318.818^{(2)}$	$318.051^{(3)}$	$318.645^{(4)}$	$318.051^{(12)}$
(100, 0)	SCSC	$147.267^{(1)}$	$88.708^{(1)}$	$82.180^{(1)}$	$81.231^{(1)}$	$81.128^{(1)}$	$81.175^{(1)}$	$81.128^{(4)}$
	SSSC	$118.597^{(1)}$	$62.617^{(1)}$	$55.371^{(1)}$	$54.050^{(1)}$	$53.796^{(1)}$	$53.778^{(1)}$	$53.796^{(4)}$
	SSSS	$118.557^{(1)}$	$59.692^{(1)}$	$49.765^{(1)}$	$47.153^{(1)}$	$46.229^{(1)}$	$45.823^{(1)}$	$45.238^{(1)}$
	SSSF	$118.539^{(1)}$	$60.704^{(1)}$	$53.002^{(1)}$	$52.025^{(1)}$	$52.165^{(1)}$	$52.473^{(1)}$	$52.025^{(5)}$
(100, 100)	SCSC	$390.532^{(1)}$	$381.956^{(1)}$	$379.360^{(2)}$	$379.926^{(3)}$	$379.889^{(3)}$	$379.360^{(4)}$	$379.414^{(14)}$
	SSSC	$338.516^{(1)}$	$328.287^{(1)}$	$325.004^{(2)}$	$325.990^{(3)}$	$325.471^{(3)}$	$325.004^{(4)}$	$325.015^{(13)}$
	SSSS	$338.517^{(1)}$	$328.223^{(1)}$	$324.996^{(2)}$	$325.988^{(3)}$	$325.451^{(3)}$	$324.996^{(4)}$	$325.005^{(13)}$
	SSSF	$338.512^{(1)}$	$328.192^{(1)}$	$324.968^{(2)}$	$325.969^{(3)}$	$325.417^{(3)}$	$324.968^{(4)}$	$324.968^{(15)}$

$R = 1$, $E_x/E_y = 2$

Table 12 Comparison of buckling load ($\bar{N}_{cr}$) from the present method with FEM results

Load case	Method	Boundary conditions			
		SCSC	SSSC	SSSS	SSSF
CASE-A	Present study	27.654	26.768	26.368	26.904
	FEM	27.632	26.703	206.411	26.897
CASE-B	Present study	53.513	51.481	51.023	51.697
	FEM	53.318	51.287	50.996	51.638
CASE-C	Present study	17.988	17.350	17.174	17.501
	FEM	17.814	17.327	17.158	17.494
CASE-D	Present study	53.927	52.564	51.308	47.017
	FEM	53.887	52.534	51.287	47.098
CASE-E	Present study	26.649	25.833	25.414	26.201
	FEM	26.588	25.830	25.403	26.318

$Q = 5, R = 2, \bar{K}_w = 10, \bar{K}_s = 100, E_x/E_y = 5$

6.3 The influence of type of loading and different combinations of boundary conditions on the critical buckling load

In Table 12, the influence of loading type on the dimensionless critical buckling load under various boundary conditions can be observed while comparing the results of the present study with those of finite element method [36].

According to Table 12, as observed, the results of finite element method have good agreement with Frobenius method' solution. As it is evident, the maximum buckling load corresponding to the state of loading CASE-D, for SCSC plate is: $\bar{N}_{cr} = 53.927$. Due to the fact that in this state of loading, a combination of tension and compression is applied to the edges, the part of the plate in tension stress improves the stability of orthotropic plate. Besides,

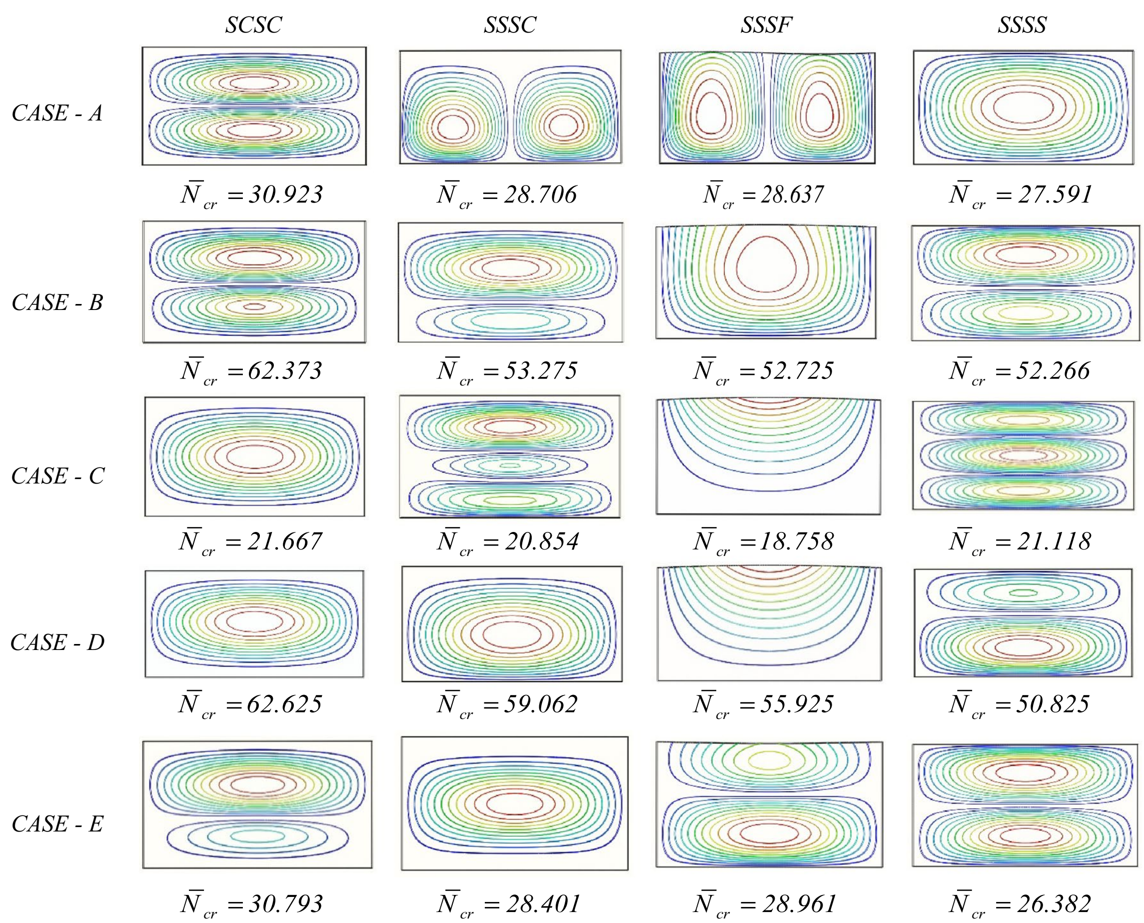

Fig. 3 The Displacement contours of plate in different cases of loading for $Q = 2,\ E_x/E_y = 10,\ R = 1,\ \bar{K}_w = 100, \bar{K}_s = 10$

the minimum critical buckling load is $\bar{N}_{cr} = 17.988$ for (CASE-C). In this case, the intensity of load on the edge $\eta = 0$, 1 is $-3N_0$. In the same loading condition, it can be found that maximum buckling load occurs for SCSC plate. On top of that, when one edge of the plate is free (there is one exception), the value of the critical buckling load gets more than that of SSSC, and SSSS plates.

7 The contours of critical buckling mode shapes

Displacement contour diagram (fixed displacement lines) of the critical buckling modes for orthotropic rectangular plate resting on Pasternak elastic foundation under biaxial in-plane loading and different boundary conditions are shown. As observed, for rectangular plate with boundary condition of SCSC (two clamped edges), the maximum and minimum buckling loads correspond to CASE-D and CASE-C, respectively (Fig. 3).

8 Conclusion

In this paper, the buckling analysis of orthotropic rectangular thin plates resting on Pasternak elastic foundation with two opposite simply supported edges, and two other edges being arbitrarily restrained, was investigated. According to Levy solution and applying Frobenius method to the governing equation, the critical buckling load of the plate was obtained. The in-plane loading was assumed to have non-uniform and nonlinear distribution. As seen, Frobenius method solution is an efficient and reliable method which presents very strong and compressed process for buckling analysis. The results showed that the accuracy of this method is dependent on the number of terms of power series for achieving convergence. Some of the important results of this study are as follows:

It is observed that by increasing the aspect ratio, in some cases, the coefficient of critical buckling load remains constant, whereas the critical buckling mode increases.

When the plate is subjected to uniaxial loading (there are a few exceptions), the values of critical buckling load get more than those in the state of biaxial loading, and occur in the higher modes.

As the value of modulus of elasticity in two different directions increases, the values of buckling load decrease.

By increasing the coefficients of elastic foundation, the values of critical buckling load grow, too. Shear foundation coefficient exerts a greater influence on the buckling load in comparison with the lateral foundation coefficient.

The buckling load of the plate is highly dependent on the type of loading at the edges.

In the specified type of in-plane loading, the maximum buckling load is allocated to that of the rectangular plate with two opposite clamped edges. Moreover, it can be found out that when the plate is under uniaxial loading, the minimum buckling load occurs when the plate has a free edge.

The results of this study can be used as a new reference to assist researchers and engineers assess the accuracy and reliability of the results and investigate the analytical and numerical methods in the future.

References

1. Ventsel E, Krauthammer T (2001) Thin plates and shells: theory, analysis and applications. Marcel Dekker Inc., New York
2. Timoshenko S.P., Gere, J.M., (1961), Theory of Elastic Stability, 2nd edn. McGraw-Hill, New York
3. Michelussi DJ (1996) Free vibration and buckling analysis of thin rectangular plates with classical boundary conditions under unilateral in-plane loads. M.Sc. thesis, Department of Mech. Eng., University of Ottawa, Ottawa
4. Kang JH, Leissa AW (2005) Exact solutions for the buckling of rectangular plates having linearly varying in-plane loading on two opposite simply supported edges. Int J Solids Struct 42:4220–4238
5. Kang JH, Leissa AW (2001) Vibration and buckling of SS-F-SS-F rectangular plates loaded by in-plane moments. Int J Struct Stab Dyn 1:527–543
6. Javaheri R, Eslami MR (2002) Buckling of functionally graded plates under inplane compressive loading. Zamm Z Angew Math Mech 82:277–283
7. Bert CW, Devarakonda KK (2003) Buckling of rectangular plates subjected to nonlinearly distributed in-plane loading. Int J Solids Struct 40:4097–4106
8. Jana P, Bhaskar K (2007) Analytical solutions for buckling of rectangular plates under non-uniform biaxial compression or uniaxial compression with in-plane lateral restraint. Int J Mech Sci 49:1104–1112
9. Jana P, Bhaskar K (2006) Stability analysis of simply-supported rectangular plates under non uniform uniaxial compression using rigorous and approximate plane stress solutions. Thin Walled Struct 44:507–516
10. Wang X, Gan L, Zhang Y (2008) Differential quadrature analysis of the buckling of thin rectangular plates with cosine-distributed compressive loads on two opposite sides. Adv Eng Softw 39(6):497–504
11. Wang X, Wang X, Shi X (2007) Accurate buckling loads of thin rectangular plates under parabolic edge compressions by the differential quadrature method. Int J Mech Sci 49(4):447–453
12. Wang X, Wang X, Shi X (2006) Differential quadrature buckling analyses of rectangular plates subjected to non-uniform distributed in-plane loadings. Thin-Walled Struct 44(8):837–843
13. Hosseini-Hashemi Sh, Khorshidi K, Amabili M (2008) Exact solution for linear buckling of rectangular Mindlin plates. J Sound Vib 315:318–342
14. Kumar Panda S, Ramachandra LS (2010) Buckling of rectangular plates with various boundary conditions loaded by non-uniform inplane loads. Int J Mech Sci 52(6):819–828

15. Latifi M, Farhatnia F, Kadkhodaei M (2013) Buckling analysis of rectangular functionally graded plates under various edge conditions using fourier series expansion. Eur J Mech A/Solids 41:16–27
16. Abolghasemi S, Eipakchi HR, Shariati M (2015) Analytical solution for buckling of rectangular plates subjected to non-uniform in-plane loading based on first order shear deformation theory. Modares Mech Eng 14(13):37–46 **(In Persian)**
17. Harris GZ (1975) The buckling of orthotropic rectangular plates, including the effect of lateral edge restraint. Int J Solids Struct 11:877–885
18. Hwang I, Lee JS (2006) Buckling of orthotropic plates under various in-plane loads. KSCE J Civ Eng 10(5):349–356
19. Lopatin AV, Morozov EV (2009) Buckling of the SSFF rectangular orthotropic plate under in-plane pure bending. Compos Struct 90:287–294
20. Lopatin AV, Morozov EV (2010) Buckling of the CCFF orthotropic rectangular plates under in-plane pure bending. Compos Struct 92:1423–1431
21. Thai H-T, Kim S-E (2011) Levy-type solution for buckling analysis of orthotropic plates based on two variable refined plate theory. Compos Struct 93:1738–1746
22. Jafari AA, Eftekhari SA (2011) An efficient mixed methodology for free vibration and buckling analysis of orthotropic rectangular plates. Appl Math Comput 218:2670–2692
23. Winkler E (1867) Die Lehre von der Elasticitaet und Festigkeit. Prag, Dominicus
24. Pasternak PL (1954) On a new method of analysis of an elastic foundation by means of two foundation constants (in Russian). In: Cosudarstrennoe Izdatelstvo Literaturi po Stroitelstvu I Arkhitekture. Moscow USSR, pp 1–56
25. Kim SM (2004) Buckling and vibration of a plate on elastic foundation subjected to in-plane compression and moving loads. Int J Solids Struct 41:5647–5661
26. Saeidifar M, Sadeghi SN, Saviz MR (2010) Analytical solution for the buckling of rectangular plates under uni-axial compression with variable thickness and elasticity modulus in the *y*-direction. Proc IMechE Part C J Mech Eng Sci 224(1):33–41
27. Akhavan H, Hosseini SH, Taher HRD, Alibeigloo A, Vahabi S (2009) Exact solutions for rectangular Mindlin plates under in-plane loads resting on Pasternak elastic foundation. Part I: buckling analysis. Comput Mater Sci 44:951–961
28. Akhavan H, Hosseini SH, Taher HRD, Alibeigloo A, Vahabi S (2009) Exact solutions for rectangular Mindlin plates under in-plane loads resting on Pasternak elastic foundation. Part II: frequency analysis. Comput Mater Sci 44:951–961
29. Hosseini-Hashemi S, Karimi M, Rokni H (2010) Hydroelastic vibration and buckling of rectangular Mindlin plates on Pasternak foundations under linearly varying in-plane loads. Soil Dyn Earthq Eng 30:1487–1499
30. Bodaghi M, Saidi AR (2011) Stability analysis of functionally graded rectangular plates under nonlinearly varying in-plane loading resting on elastic foundation. Arch Appl Mech 81:765–780
31. Panahandeh-Shahraki D, Amiri Rad A (2014) Buckling of cracked functionally graded plates supported by Pasternak foundation. Int J Mech Sci 88:221–231
32. Foroughi H, Azhari M (2014) Mechanical buckling and free vibration of thick functionally graded plates resting on elastic foundation using the higher order B-spline finite strip method. Meccanica 49:981–993
33. Yaghoobi H, Fereidoon A (2014) Mechanical and thermal buckling analysis of functionally graded plates resting on elastic foundations: an assessment of a simple refined nth-order shear deformation theory. Compos Part B Eng 62:54–64
34. Viswanathana KK, Navaneethakrishnan PV (2015) Buckling analysis of rectangular plates with variable thickness resting on elastic foundation. IOP Conf Ser Earth Environ Sci 23:012006
35. Lam K, Wang C, He X (2000) Canonical exact solutions for Levy-plates on two-parameter foundation using Green's functions. Eng Struct 22:364–378
36. Shahraki H (2015) Buckling analysis of orthotropic rectangular plates subjected to bi-axial non-uniformly in-plane loading resting on Pasternak foundation. MSc. thesis (in Persian), Islamic Azad University, Khomeinishahr Branch